Molecular Crystals and Liquid Crystals

Publication details, including instructions for authors and subscription information:
http://www.tandfonline.com/loi/gmcl20

Subharmonic Pattern Formation in a Nematic Cell - A 1D Flexoelectric Model Approach

Jonathan Low [a] & S. John Hogan [a]

[a] Bristol Centre for Applied Nonlinear Mathematics, Department of Engineering Mathematics, University of Bristol, Bristol, UK

Version of record first published: 22 Sep 2010

To cite this article: Jonathan Low & S. John Hogan (2007): Subharmonic Pattern Formation in a Nematic Cell - A 1D Flexoelectric Model Approach, Molecular Crystals and Liquid Crystals, 478:1, 67/[823]-81/[837]

To link to this article: http://dx.doi.org/10.1080/15421400701735640

Mol. Cryst. Liq. Cryst., Vol. 478, pp. 67/[823]–81/[837], 2007

ISSN: 1542-1406 print/1563-5287 online
DOI: 10.1080/15421400701735640

Taylor & Francis
Taylor & Francis Group

Subharmonic Pattern Formation in a Nematic Cell – A 1D Flexoelectric Model Approach

Jonathan Low
S. John Hogan
Bristol Centre for Applied Nonlinear Mathematics, Department of Engineering Mathematics, University of Bristol, Bristol, UK

The application of an AC electric field to a nematic liquid crystal cell produces two distinct instability pattern regimes, conductive or dielectric. Recently, asymmetric electric field waveforms have been shown to cause a period-doubling subharmonic bifurcation. We extend these calculations to include flexoelectricity in the one-dimensional case. We calculate the threshold values for the electric field strength determining the optimum oblique angle at which the roll patterns form. We find, in some areas of parameter space, the formation of oblique rolls is favoured over normal rolls. In addition we find cross-over points from normal to oblique rolls called Lifshitz points. These have been found in the subharmonic and dielectric regions of the linear stability diagram.

Keywords: Carr-Helfrich; electrohydrodynamic instability; flexoelectricity; nematic; pattern formation; subharmonic dynamics

1. INTRODUCTION

Nematic electroconvection is an example of a pattern-forming system [1] where the influence of an alternating electric field on a liquid crystal cell causes the thread-like molecules to undergo periodic modulation together with ionic charge separation. At a critical electric field strength, the formation of Williams domains [2] occurs which is easily observed under a light microscope due to the nematic's

One of the authors, Jonathan Low, wishes to thank the Engineering and Physical Sciences Research Council (EPSRC) UK for funding and to thank Ralf Stannarius for both Mischung V liquid crystal data and for a visit to his research group in Magdeburg, Germany.

Address correspondence to Jonathan Low, Bristol Centre for Applied Nonlinear Mathematics, Department of Engineering Mathematics, University of Bristol, Queen's Building, Bristol, BS8 1TR, UK. E-mail: j.low@bristol.ac.uk

birefringent properties. The theory describing this type of dynamics had been put forward by Carr [3] and Helfrich [4]. This happens for a nematic with a negative dielectric anisotropic value ($\epsilon_a < 0$) and a positive conductivity value ($\sigma_a > 0$).

This kind of pattern formation had been studied under static DC fields [5], whereby a static distortion of the director fields can be obtained by using a static electric field to the liquid crystal cell, provided the field strength is above a certain threshold. An introduction to this can be found in a review by Stephen [6] and by Chandrasekhar [7]. This DC instability was studied by Raghunathan [8] with the flexoeffect. Theoretical and experimental studies then moved on to systems under AC field excitation. de Gennes [9] from the Orsay group developed a simple 1D model with AC driving. This was followed by Langerwall [10] with a detailed analytical treatment with simple AC square waves. The Orsay group used electric field waveforms in which the solution propagation could not be expressed analytically. On the other hand, Langerwall, through a simple symmetric square wave excitation, made analytical progress in terms of explicit expressions for the eigenvalues (Floquet multipliers) of the evolution operator or fundamental matrix to determine the parameter regions where the two different types of dynamics (conduction or dielectric regimes) occur. A 3D model was analysed [11], resulting in the possible formation of roll instability at an oblique angle as opposed to normal rolls in the previous models. But Madhusudana extended the 1D system to include flexoelectricity [12], which also resulted in oblique rolls, in regions of the conductive and dielectric curves. They used the simple square wave excitation as Langerwall [10], and found that oblique rolls were the favoured first instability, which explained some observations that calculated threshold values were not the same as those obtained in experiment. Such examples of experiments observing the formation of oblique roll paterns have been done by Joets [13]. A description of the influence of flexoelectricity on electroconvection can be found in Chandrasekhar [7].

Usually, the waveforms of these excitation electric fields have been symmetric. More recently, a new type of patterm regime was discovered using an asymmetric excitation field [14]. Compared to both the classical conductive and dielectric modes, this 'subharmonic' regime sees both the director and excess charge change sign after one period of the excitation field. The shape of the electric field waveform is one of the important conditions for this subharmonic response. John and Stannarius [14] used an asymmetric piecewise constant field. Later on, experimental and numerical studies were performed using variable triangular waveforms for the electric field [15] and then

further analysis on the existence of subharmonic dynamics in electroconvection was carried out [16].

The aim of this article is to apply the methodology used by Madhusudana [12] using the same asymmetric piecewise constant field [14] in order to study the effect of flexoelectricity on the subharmonic patterns. The paper is divided up into three sections. Section 2 contains the mathematical formulation we will be using and its justification. In section 3, the results are computed for the 1D model with flexoelectricity for the purpose of determining the threshold values of the electric field strength at which the system destabilises into roll formation. In addition, results that have been computed from past work are shown here. Section 4 contains a summary.

2. MATHEMATICAL FORMULATION

Figure 1 defines the coordinate system for the problem. The Cartesian axes *xyz* are related to the boundaries of the liquid crystal cell and the AC field acts parallel to the *z*-axis everywhere. We can physically think of the *xy*-plane being parallel to the glass plates of a nematic liquid crystal cell with the origin between the two plates. ***n*** represents the director field which describes the general orientation of the nematic thread at a given point in space and time. $\phi(t)$ and $\vartheta(t)$ are the angles from the *xy*-plane and *xz*-plane respectively which are used

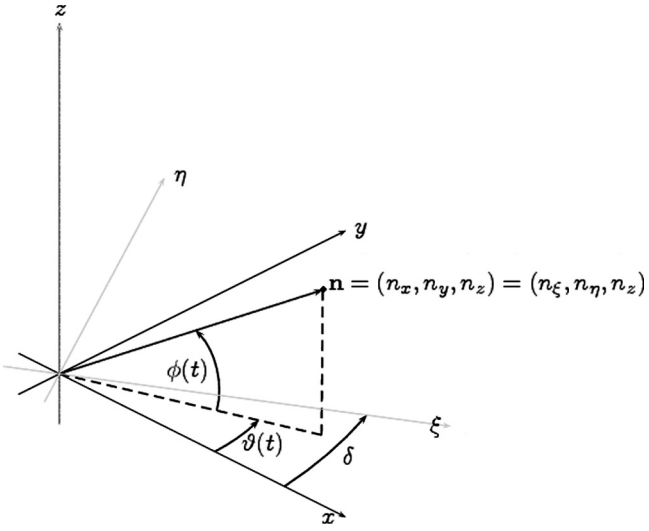

FIGURE 1 Definition of coordinate system used.

to describe the direction of the director. The flexoeffect will produce rolls oblique to the x-axis. Hence we rotate the axes through an angle δ about the z-axis to account for this and all expressions will be in relative to that frame. The horizontal wave vector will be along the axis ξ.

We give the main equations in component form following Mullin [17] who also uses the convenient Einstein index notation. The full non-linear equations are found in the book by Stewart [18] and are composed of the Ericksen-Leslie dynamic equations together with Maxwell's equations. The notation used throughout this paper is the same as in the book except for the Miesowitz viscosities where we use the Helfrich notation (η_1 and η_2 interchange their definitions):

$$\eta_1 = \frac{1}{2}(-\alpha_2 + \alpha_4 + \alpha_5)$$

$$\eta_2 = \frac{1}{2}(\alpha_2 + 2\alpha_3 + \alpha_4 + \alpha_5)$$

where the α_i are the Leslie viscosity coefficients.

The Ericksen-Leslie equations describing the motion of the director and fluid flow are given by:

$$v_{p,p} = 0 \tag{2.1}$$

$$n_p n_p = 1 \tag{2.2}$$

$$\rho \frac{\mathrm{D}v_i}{\mathrm{D}t} = \rho F_i - (p + w_F)_{,i} + \tilde{g}_j n_{j,i} + G_j n_{j,i} + \tilde{t}_{ij,j} \tag{2.3}$$

$$\left(\frac{\partial w_F}{\partial n_{i,j}}\right)_{,j} - \frac{\partial w_F}{\partial n_i} + \tilde{\boldsymbol{g}}_i + G_i = \lambda n_i \tag{2.4}$$

where $\mathbf{v}$ is the velocity field of the liquid crystal, ρ is the nematic density, $\mathbf{F}$ is the bulk force per unit mass, p is the pressure, $\tilde{\mathbf{g}}$ is a dynamic term related to torque forces, $\mathbf{G}$ is the generalised body force, $\tilde{t}$ is the stress tensor, λ is the Lagrange multiplier arising from the constraint (2.2) and w_F is the Frank-Oseen elastic energy for nematics given by

$$w_F = \frac{1}{2}K_1(\nabla \cdot \boldsymbol{n})^2 + \frac{1}{2}K_2(\boldsymbol{n} \cdot \nabla \times \boldsymbol{n})^2 + \frac{1}{2}K_3(\boldsymbol{n} \times \nabla \times \boldsymbol{n})^2 - \frac{\epsilon_\mathrm{a}}{8\pi}(\boldsymbol{n} \cdot \boldsymbol{E})^2 - \boldsymbol{P} \cdot \boldsymbol{E} \tag{2.5}$$

where the K_i ($i = 1, 2, 3$) are the Frank elastic coefficients of splay, twist and bend respectively and $\boldsymbol{E}$ is the applied electric field. Equation (2.1) is the incompressiblity condition, (2.2) ensures that $\boldsymbol{n}$

remains a unit vector, and Eqs. (2.3) and (2.4) are the equations of linear and angular momentum respectively. The bulk force due to the electric effects is given by $\rho F_i = qE_i$ where q is the charge density.

The term $\boldsymbol{P}\cdot\boldsymbol{E}$ is the additional term to account for the flexoeffect and $\boldsymbol{P}$ has the form:

$$P_i = e_1 n_i (n_{p,p}) + e_3 n_k [n_{i,k} - n_{k,i}] \tag{2.6}$$

where e_1 and e_3 are the flexoelectric coefficients. The flexoeffect adds an extra polarisation term to the electric displacement $\mathbf{D}$ and an extra energy in the Frank elastic energy, which is the $\boldsymbol{P}\cdot\boldsymbol{E}$ term in Eq. (2.5). This results in new terms involving the flexoelectric coefficients e_1 and e_3, which always appear in the combinations $(e_1 \pm e_3)$. The physical interpretation of flexoelectricity is that an internal electric field is created when a line of nematic threads undergoes a splay or bend deformation, creating an unequal internal field inside. This is the extra polarisation that is added into the model. Hence the physical interpretation of e_1 and e_3 is the amount of internal field generated with respect to splay and bend deformation respectively. By symmetry, no internal field is possible under a twist deformation. We supplement the Ericksen-Leslie equations with Maxwell's equations to fully incorporate the electrical effects into the system. This includes conservation of charge and current movement. We make the quasi-static approximation [19] so that the equations become:

$$D_{p,p} = 4\pi q \tag{2.7}$$

$$\varepsilon_{ijk} \frac{\partial E_k}{\partial x_j} = 0 \tag{2.8}$$

$$\frac{Dq}{Dt} + J_{p,p} = 0 \tag{2.9}$$

together with the relations

$$D_i = \epsilon_{ij} E_j + 4\pi P_i \quad \text{and} \quad J_i = \sigma_{ij} E_j \tag{2.10}$$

where $\mathbf{D}$ is the electric displacement, $\mathbf{J}$ is the current density and ϵ_{ij} and σ_{ij} are the dielectric and conductivity tensors of the uniaxial nematic form:

$$\beta_{ij} = \beta_\perp \delta_{ij} + \beta_a n_i n_j \tag{2.11}$$

$$= \beta_\perp \delta_{ij} + (\beta_\parallel - \beta_\perp) n_i n_j \tag{2.12}$$

with δ_{ij} the Kronecker delta and $\beta_\perp$ and $\beta_\parallel$ are the material parameters perpendicular and parallel to the nematic thread respectively. Equation (2.8) contains the alternating tensor ε_{ijk} which takes the value 1 for even permutations, -1 for odd permutations and 0 otherwise. Equations (2.1–2.4), (2.7–2.9) are the basic equations of our system. We now proceed to analyse them. The basic null state is mathematically represented by a uniform homogeneous director alignment together with no charge, no flow field and current movement acting only perpendicular on the director, namely

$$\boldsymbol{n}_0 = (n_x = 1, n_y = 0, n_z = 0) \tag{2.13}$$

$$= (n_\xi = \cos(\delta), n_\eta = \sin(\delta), n_z = 0) \tag{2.14}$$

$$q_0 = 0 \tag{2.15}$$

$$\mathbf{v}_0 = 0 \tag{2.16}$$

$$\mathbf{E}_0 = (0, 0, E(t)) \tag{2.17}$$

$$\mathbf{J}_0 = \sigma_\perp \mathbf{E}_0(t) \tag{2.18}$$

where $E(t)$ is the applied electric field.

This basic state is then subjected to small perturbations $\boldsymbol{n_1}$, q_1, $\mathbf{v_1}$ and $\mathbf{E_1}$. The director is perturbed at small angles $\phi(t)$ and $\vartheta(t)$. Hence the director field is linearised as follows:

$$\begin{aligned}\boldsymbol{n}_1 &= [\cos(\phi(t))\cos(\delta - \psi(t)), -\cos(\phi(t))\sin(\delta - \psi(t)), \sin(\phi(t))] \\ &\approx [\cos(\delta) + \sin(\delta)\vartheta(\xi, t), \cos(\delta)\vartheta(\xi, t) - \sin(\delta), \varphi(\xi, t)]\end{aligned}$$

using double angle formulae and the fact that $\phi(t) \ll 1$ and $\vartheta(t) \ll 1$.

Normal roll formation is attained for $\delta = 0$ in which the x and ξ axes coincide, and oblique rolls for $\delta \neq 0$. The linearised electrohydrodynamic equations are derived by using the following test mode ansatz for the perturbation, which will test the basic null state of the liquid crystal cell against the formation of rolls:-

$$q_1(\xi, t) = \tilde{\boldsymbol{q}}_1(t)\cos(k_\xi \cdot \xi), \tag{2.19}$$

$$\phi(\xi, t) = \tilde{\boldsymbol{\phi}}(t)\cos(k_\xi \cdot \xi), \tag{2.20}$$

$$\psi(\xi, t) = \frac{\partial \phi}{\partial \xi} = \tilde{\boldsymbol{\psi}}(t)\sin(k_\xi \cdot \xi), \tag{2.21}$$

$$\vartheta(\xi, t) = \tilde{\vartheta}(t)\sin(k_\xi \cdot \xi), \tag{2.22}$$

$$E_\xi(\xi, t) = \widetilde{E}_{\text{ind}}(t)\cos(k_\xi \cdot \xi), \tag{2.23}$$

$$v_z(\xi, t) = \tilde{v}_z(t)\sin(k_\xi \cdot \xi), \tag{2.24}$$

$$p_1(\xi, t) = \tilde{p}(t)\sin(k_\xi \cdot \xi). \tag{2.25}$$

where k_ξ is the wavenumber in the ξ direction.

Substituting Eqs. (2.19)–(2.25) into (2.1)–(2.10) we obtain the following 3×3 system upon linearisation[1]:

$$\begin{pmatrix} \dot{q}_1 \\ \dot{\psi} \\ \dot{\vartheta} \end{pmatrix} + \begin{pmatrix} \frac{1}{T_q} & \sigma_H E(t) & \frac{q_\vartheta}{T_q} \\ aE(t) & \Lambda_1 - \Lambda_2 E^2(t) & bE(t) \\ \frac{e_q}{\gamma_1} & \frac{e_\psi}{\gamma_1} E(t) & \frac{1}{T_\vartheta} \end{pmatrix} \begin{pmatrix} q_1 \\ \psi \\ \vartheta \end{pmatrix} = \begin{pmatrix} 0 \\ 0 \\ 0 \end{pmatrix} \tag{2.26}$$

where the coefficients [12,20] in the matrix are constants depending on the material parameters, wavenumber and the oblique angle δ. Some of the coefficients are explicitly coupled to the electric field strength $E(t)$ as shown above. The advantage of a constant piecewise field is that it allows for the analytical calculation of the evolution matrix and the Floquet multipliers of the system.

3. RESULTS AND CALCULATIONS

3.1. Solution Method

System (2.26) is solved using Floquet theory since the electric field $E(t)$ is periodic. The waveform of the field is the same asymmetric piecewise constant field used by John in his work [14] and is shown in Figure 2.

One calculates, for a given wavenumber k_ξ and oblique roll angle δ, the eigenvalues of the fundamental matrix, consisting of eight matrix exponentials chained together (one for each piecewise constant section of $E(t)$). The basic null state is then stable for all eigenvalues less than one in modulus. The system bifurcates to a harmonic response if the largest Floquet multiplier in modulus crosses $+1$, and a period-doubling response occurs if it crosses -1. For material parameters, we use the published values of MBBA [8,21] for the model with the symmetric square wave electric field, and Mischung V [14] for the model with the asymmetric electric field. For material parameters

[1]Dropping the tildas for convenience.

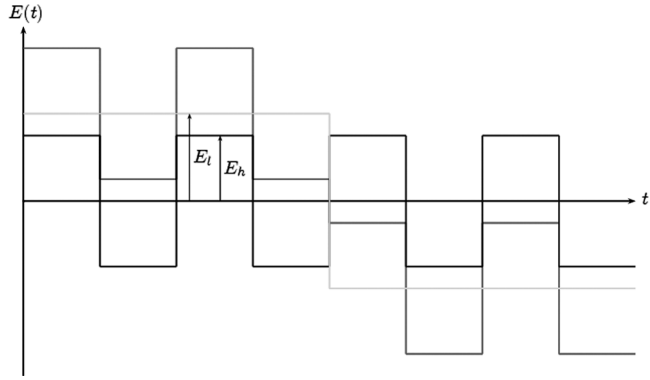

FIGURE 2 One full period of the waveform $E(t)$. This is composed of a superposition of two square waves, one with amplitude E_l at 80 Hz and another with amplitude E_h at 320 Hz.

not known in Mischung V, (α_4 α_5 and K_2), we approximate α_4 using the tabulated data by Shi *et al*. [22] and then calculate the theoretical value for α_5 from that, which satisfies the equation for the Miesowitz viscosity

$$\eta_1 = \frac{1}{2}(\alpha_4 + \alpha_5 - \alpha_2)$$

using the α_2 calculated from Stannarius's γ_1 and γ_2 values for Mischung V. The K_2 value was provided by experimental work from Stannarius (personal communication) based on finding the twist Freedericksz threshold values. For flexoelectricity, we have taken the approach of exploring what changes would occur if this effect were included. Hence, although the real value for Miscung V may be smaller than that for MBBA, we have taken the same values as a 'first try'. One can also view this as a way of finding out the difference for any nematic liquid crystal with similar material property values. The list of parameters[2] used in this article are given in Table 1.

3.2. Wavenumber Selection

There is the issue of mode selection when using the 1D model. This is certainly a problem in the conduction regime, where $k_\xi = 0$ gives the lowest threshold. A physical explanation is found in Langerwall [10]. The approach we decided to take is whenever a wavenumber lower

[2]Conversion between SI and cgs units is done using conversion tables found in Jackson [23] and Stewart [18].

TABLE 1 Parameters and Quantities Used in the Calculation of the Stability Diagram

Quantity	Mischung V values (cgs units)	MBBA values (cgs units)
$\epsilon_\parallel$	5.6	4.5
$\epsilon_\perp$	6.0	5.0
$\epsilon_a = \epsilon_\parallel - \epsilon_\perp$	-0.4	-0.5
$\sigma_\parallel$	$260\,\mathrm{s}^{-1}$	$270\,\mathrm{s}^{-1}$
σ	1.5	1.5
$\sigma_\perp = \dfrac{\sigma_\parallel}{\sigma}$	$173\frac{1}{3}\,\mathrm{s}^{-1}$	$180\,\mathrm{s}^{-1}$
$\sigma_a = \sigma_\parallel - \sigma_\perp$	$86\frac{2}{3}\,\mathrm{s}^{-1}$	$90\,\mathrm{s}^{-1}$
η_1	$4\,\mathrm{g\,cm}^{-1}\,\mathrm{s}^{-1}$	$1.035\,\mathrm{g\,cm}^{-1}\,\mathrm{s}^{-1}$
η_2	$0.4\,\mathrm{g\,cm}^{-1}\,\mathrm{s}^{-1}$	$0.238\,\mathrm{g\,cm}^{-1}\,\mathrm{s}^{-1}$
γ_1	$3.67\,\mathrm{g\,cm}^{-1}\,\mathrm{s}^{-1}$	$0.763\,\mathrm{g\,cm}^{-1}\,\mathrm{s}^{-1}$
$\gamma_2 = -\gamma_1$	$-3.67\,\mathrm{g\,cm}^{-1}\,\mathrm{s}^{-1}$	$-0.788\,\mathrm{g\,cm}^{-1}\,\mathrm{s}^{-1}$
α_1	$0.2\,\mathrm{g\,cm}^{-1}\,\mathrm{s}^{-1}$	$0.065\,\mathrm{g\,cm}^{-1}\,\mathrm{s}^{-1}$
α_2	$-3.67\,\mathrm{g\,cm}^{-1}\,\mathrm{s}^{-1}$	$0.775\,\mathrm{g\,cm}^{-1}\,\mathrm{s}^{-1}$
α_4	$1.51\,\mathrm{g\,cm}^{-1}\,\mathrm{s}^{-1}$	$0.463\,\mathrm{g\,cm}^{-1}\,\mathrm{s}^{-1}$
α_5	$2.82\,\mathrm{g\,cm}^{-1}\,\mathrm{s}^{-1}$	$0.832\,\mathrm{g\,cm}^{-1}\,\mathrm{s}^{-1}$
K_1	$14.90 \times 10^{-7}\,\mathrm{g\,cm\,s}^{-2}$	$6.1 \times 10^{-7}\,\mathrm{g\,cm\,s}^{-2}$
K_2	$6.48 \times 10^{-7}\,\mathrm{g\,cm\,s}^{-2}$	$4.0 \times 10^{-7}\,\mathrm{g\,cm\,s}^{-2}$
K_3	$13.76 \times 10^{-7}\,\mathrm{g\,cm\,s}^{-2}$	$7.3 \times 10^{-7}\,\mathrm{g\,cm\,s}^{-2}$
Cell thickness d	20.2×10^{-4} cm	20.2×10^{-4} cm
e_1	-2.9×10^{-4} statcoulombs cm^{-1}	-2.9×10^{-4} statcoulombs cm^{-1}
e_3	-4.1×10^{-4} statcoulombs cm^{-1}	-4.1×10^{-4} statcoulombs cm^{-1}

than π/d gives a lower threshold, we take the threshold value at $k_\xi = \pi/d$. This is commonly referred to as the Helfrich condition.

3.3. Results and Comments

The results of our numerical calculations are shown in Figures 3 to 10. Figure 3 shows the classical result of the conductive and dielectric regimes as the amplitude and frequency of the square wave electric field are varied[3]. Both regimes are clearly indicated. The distinct features, such as the S-shape curve and the conduction cut-off frequency, are similar to that of Dubois-Violette [24]. Figure 4 is the result found by Madhusudana [12] and shows the threshold values when flexoelectricity is added to the model. The dashed lines indicate that, for a nonzero oblique angle δ, a more favourable threshold value is found over the value for normal roll formation. Again both the conduction and dielectric regimes are clearly marked. Dashed lines (a) and (b) are the threshold curves for oblique rolls which are lower than those

[3]The 3×3 matrix of coefficients is now reduced to the 2×2 matrix [10].

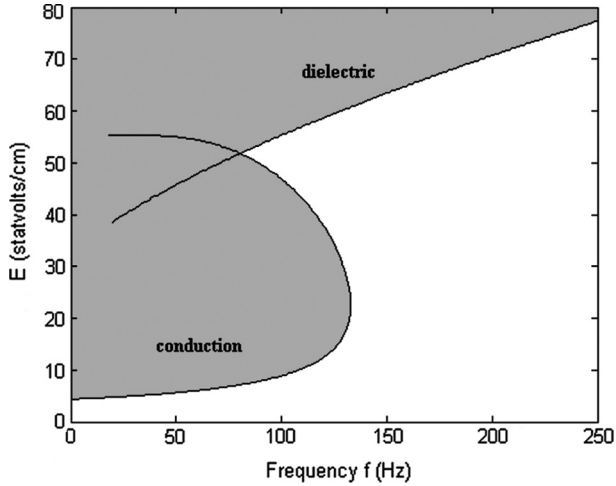

FIGURE 3 Stability thresholds for square wave excitation (without flexoelectricity).

for normal rolls. Line (c) is where *higher* thresholds are found compared to those for normal rolls. The points where (a) and (c) cross the solid line are the Lifshitz points. This curve gives a larger

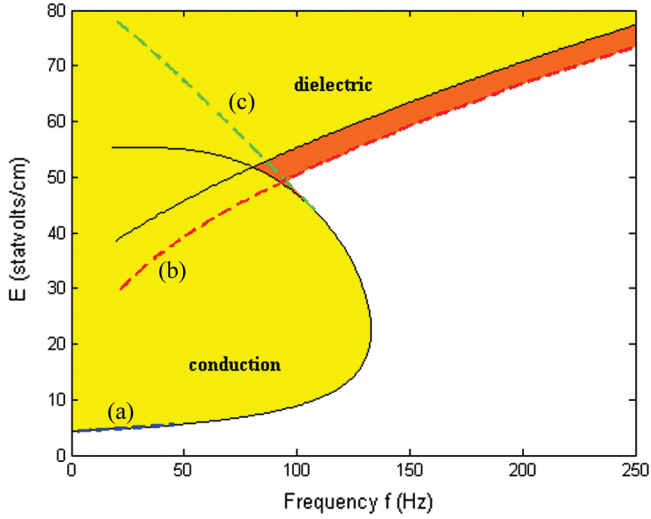

FIGURE 4 Stability thresholds for square wave excitation (with flexoelectricity).

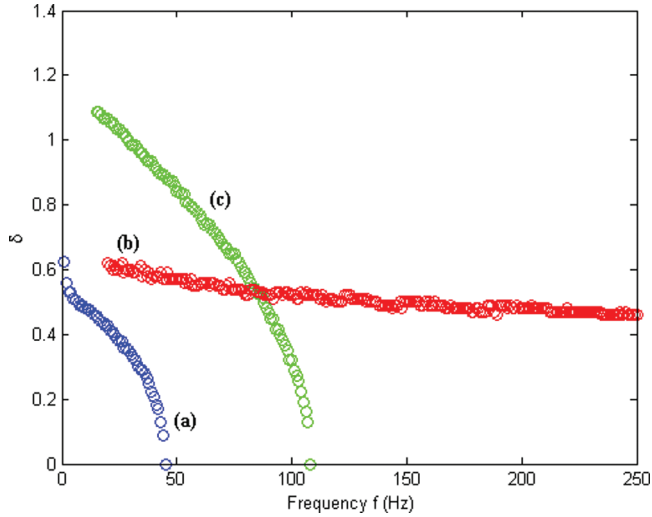

FIGURE 5 Angle of oblique rolls as a function of frequency at stability threshold for square wave excitation (with flexoelectricity).

conduction regime area than the curve produced by the model without flexoelectricity. Figure 5 shows the corresponding oblique angle δ for the curves (a), (b) and (c).

The threshold diagram when $E(t)$ is the asymmetric field shown in Figure 2, using the model without flexoelectricity, is in Figure 6. Here we fix the frequencies of the excitation as given in Figure 2, plot the instability boundaries in the (E_1, E_h) plane, and label the three regions where the conduction, subharmonic and dielectric solutions occur. When flexoelectricity is added, the results are shown in Figures 7 and 8. The dashed lines mark the low frequency field amplitude values where a non-zero oblique angle causes the threshold to be lower than for normal rolls. Note that the S-shape in the conduction-subharmonic area is eliminated and covered where the dashed conduction line meets the black subharmonic line, and the Lifshitz points are present on the subharmonic and dielectric curves.

Figures 9 and 10 show the dynamics at a threshold point without and with flexoelectricity respectively, over two periods of the electric field cycle in the subharmonic regime. The low frequency electric field chosen was $E_1 = 77$ statvolts/cm. In both figures, the electric field amplitude has been scaled down by a factor of 220. Both the charge q_1 and director deflection ψ change signs over one period of the electric field. The variable ϑ in Figure 10 is virtually zero, whereas q and ψ

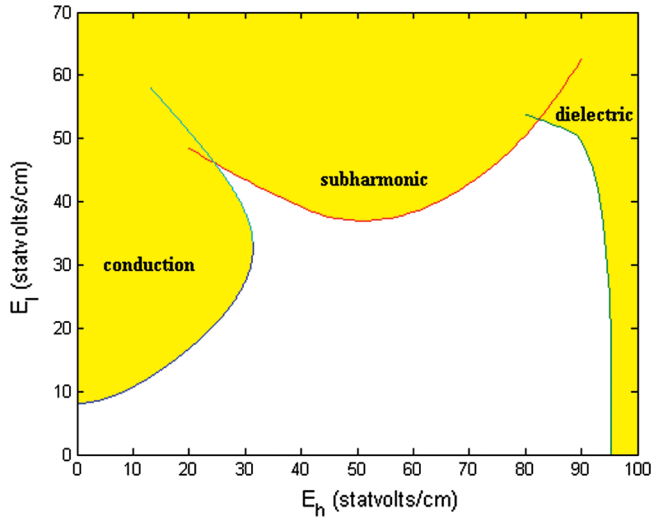

FIGURE 6 Stability thresholds for asymmetric excitation (without flexoelectricity).

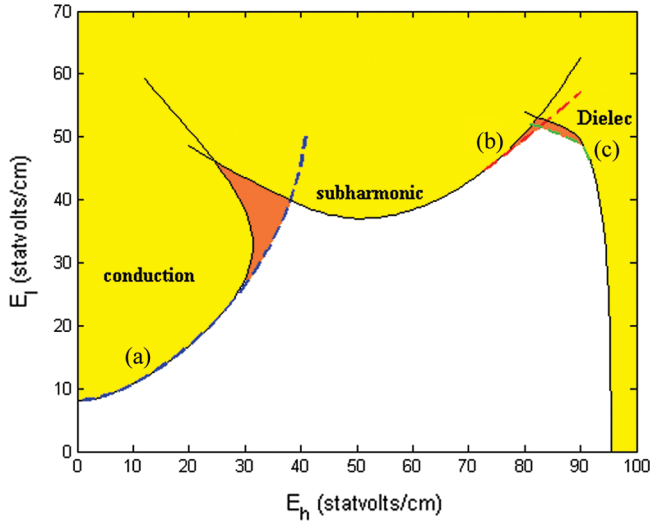

FIGURE 7 Stability thresholds for asymmetric excitation (with flexoelectricity).

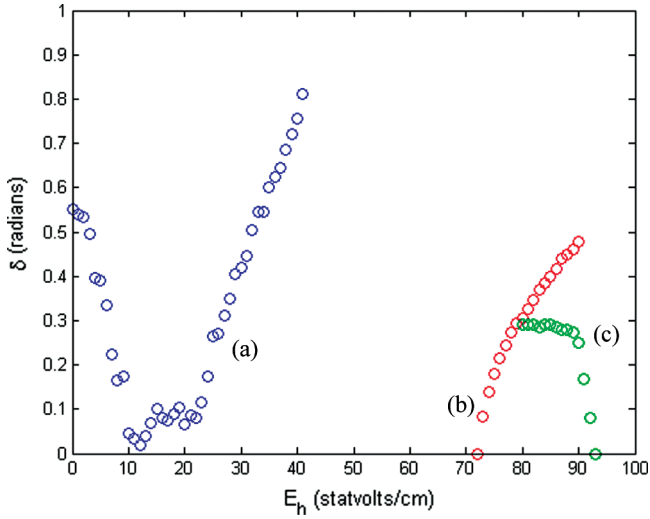

FIGURE 8 Angle of oblique rolls at stability threshold for asymmetric excitation (with flexoelectricity).

reach large values (which challenge the assumption that the system variables are small). Overall, there appears to be little difference between the two figures, except that the dynamics for the variables

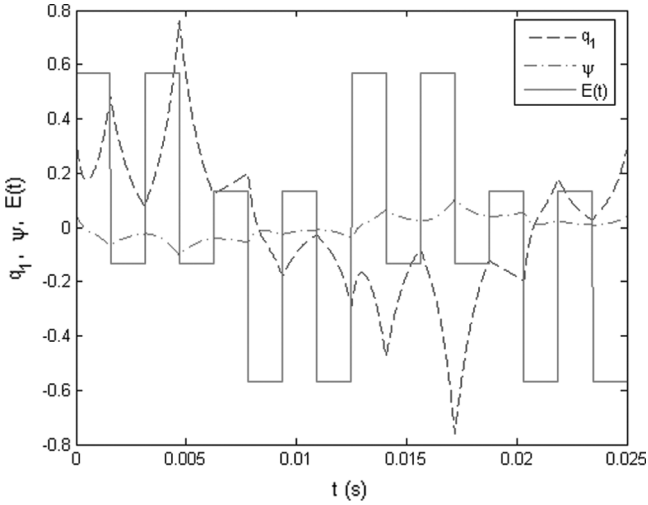

FIGURE 9 Dynamics over the electric field cycle (without flexoelectricity).

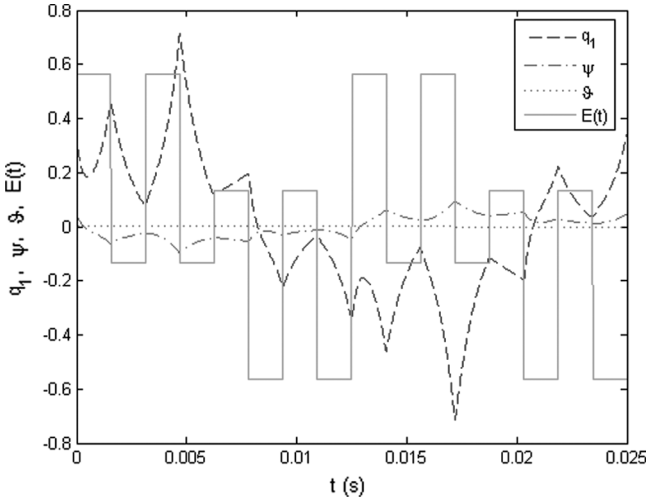

FIGURE 10 Dynamics over the electric field cycle (with flexoelectricity).

shown in Figure 7 are happening at an oblique angle δ (about 0.25 in this case) from the horizontal x-axis. Labels (a), (b) and (c) in Figures 7 and 8 are used in the same way as for Figures 4 and 5.

Hence we conclude that the lowering of the threshold values due to a non-zero δ angle is possible where we vary the amplitudes of the two electric fields. This is due to the flexoelectric contribution that can alter the point at which the first instability occurs.

4. SUMMARY

We have shown, using a linear stability analysis of the electrohydrodynamic equations with the flexoeffect in a 1D setting, that the threshold values where the first instability occurs are lowered further when the inclusion of an oblique angle parameter δ is included in the system, giving us an extra degree of freedom. The 3×3 coupled ODE system is derived from the full hydrodynamic equations with Maxwell's equations using a roll ansatz. MATLAB codes were checked by reproducing published results as shown before. The main conclusion from this study is the alteration of threshold values due to a non-zero δ.

This theory cannot be used to model higher instabilities beyond the threshold. One needs to go back to the full nonlinear equations and seek the next stable solution. The next step beyond linear stability is to examine the non-linear effects [25] or the analytical manipulation of amplitude equations. This has been extensively researched by

Kramer and others [19,26] before subharmonic dynamics were discovered in this pattern-forming system.

REFERENCES

[1] Buka, A. & Kramer, L. (Eds.) (1996). *Pattern Formation in Liquid Crystals*, Springer: New York, USA.
[2] Williams, R. (1963). *J. Chem. Phys.*, *39*, 384.
[3] Carr, E. F. (1969). *Mol. Cryst. Liq. Cryst.*, *7*, 253.
[4] Helfrich, W. (1969). *J. Chem. Phys.*, *51*, 4092.
[5] Penz, P. A. & Ford, G. W. (1972). *Phys. Rev. A*, *6*, 414.
[6] Stephen, M. J. & Straley, J. P. (1974). *Rev. Mod. Phys.*, *46*, 617.
[7] Chandrasekhar, S. (1992). *Liquid Crystals*, CUP: Cambridge, UK, Chapter 3, 85.
[8] Madhusudana, N. V., Raghunathan, V. A., & Sumathy, K. R. (1987). *Pramana J. Phys.*, *28*, L311.
[9] de Gennes, P. G., Dubois-Violette, E., & Parodi, O. (1971). *J. Phys. (France)*, *32*, 305.
[10] Langerwall, S. T., Dubois-Violette, E., Smith, I. W., Galerne, Y., & Durand, G. (1975). *J. Phys. (France)*, *36*, C1–237.
[11] Zimmermann, W. & Kramer, L. (1985). *Phys. Rev. Lett.*, *55*, 402.
[12] Madhusudana, N. V. & Raghunathan, V. A. (1998). *Mol. Cryst. Liq. Cryst. Lett.*, *5*, 201.
[13] Joets, A., Ribotta, R., & Lei, L. (1986). *Phys. Rev. Lett.*, *56*, 1595.
[14] John, T. & Stannarius, R. (2004). *Phys. Rev. E*., *70*, 025202(R).
[15] Heuer, J., Stannarius, R., & John, T. (2005). *Phys. Rev. E*., *71*, 056307.
[16] Heuer, J., Stannarius, R., & John, T. (2005). *Phys. Rev. E*., *72*, 066218.
[17] Tavener, S. J., Mullin, T., Blake, G. I., & Cliffe, K. A. (2000). *Phys. Rev. E*., *63*, 011708.
[18] Stewart, I. W. (2004). *The Static and Dynamic Continuum Theory of Liquid Crystals*, Taylor and Francis: London, UK.
[19] Kramer, L., Bodenschatz, E., Pesch, W., Thom, W., & Zimmermann, W. (1989). *Liq. Cryst.*, *5*, 699.
[20] Lange, A., Müller, R., & Behn, U. (1996). *Z. Phys. B*., *100*, 477.
[21] Lange, A., Behn, U., & John, T. (1998). *Phys. Rev. E*., *58*, 2047.
[22] Shi, J., Wang, C., Surendranath, V., Kang, K., & Gleeson, J. T. (2002). *Liq. Cryst.*, *29*, 877.
[23] Jackson, J. D. (1998). *Classical Electrodynamics*, Wiley: New York.
[24] Dubois-Violette, E. (1972). *J. Phys. (France)*, *33*, 95.
[25] Brand, H. R. & Pleiner, H. (1987). *Phys. Rev. A*, *35*, 3122.
[26] Kaiser, M. & Pesch, W. (1993). *Phys. Rev. E*., *48*, 4510.